

Photonic band structure and symmetry properties of electromagnetic modes in photonic crystals

S. B. Cavalcanti,^{1,2} M. de Dios-Leyva,^{3,4} E. Reyes-Gómez,⁴ and L. E. Oliveira²

¹*Instituto de Física, Universidade Federal de Alagoas, Maceió-AL, 57072-970, Brazil*

²*Instituto de Física, Universidade Estadual de Campinas—UNICAMP, CP 6165, Campinas—SP, 13083-970, Brazil*

³*Department of Theoretical Physics, University of Havana, San Lázaro y L, Vedado 10400, Havana, Cuba*

⁴*Instituto de Física, Universidad de Antioquia, AA 1226, Medellín, Colombia*

(Received 14 November 2006; published 12 February 2007)

Within the Maxwell framework and using a transfer-matrix technique we have determined a general equation which governs the photonic band structure and the density of states of one-dimensional superlattices composed of two alternate layers characterized by different refractive indexes, which may take on positive as well as negative values. Besides the usual well-known results, we have found null-gap points for commensurate values of the optical path lengths of each layer. Furthermore, we have been able to characterize non-Bragg gaps that show up in frequency regions in which the average refractive index is null.

DOI: [10.1103/PhysRevE.75.026607](https://doi.org/10.1103/PhysRevE.75.026607)

PACS number(s): 42.70.Qs, 42.70.Gi

I. INTRODUCTION

Since the pioneering work of Yablonovitch [1] and John [2], many experimental and theoretical works have been devoted to the study of the physical properties of photonic crystals (PCs), which are artificial periodic arrays of materials with different refractive indices. This interest is motivated by the new perspective that such structures provide us in our ability to control the properties of light, leading to a new era of optical devices. The rapidly developing realm of PCs, however, abounds with challenges, both theoretical and experimental, and most of these are derived from the fact that these artificially, composite systems exhibit photonic band gaps (PBG) in much the same fashion as electrons in semiconductors, in the sense that they produce frequency ranges for which light propagation is prohibited [3,4]. Among the most striking effects of the existence of PBGs are the inhibition [5] and enhancement of spontaneous emission for atomic systems embedded in PCs as a consequence of externally controllable entangled atom-photon states that are originated when the atomic frequency is tuned in the vicinity of the band gap, leading to non-Markovian effects [6]. Another very interesting application of PCs is connected with the fact that nowadays they might be engineered to exhibit negative refractive index. The theoretical idea, first proposed by Veselago [7], has been realized via a successful artificial material whose unit cell consists of a combination of a wire with the so-called split-ring resonator (SRR) which, in spite of being nonmagnetic, exhibit negative magnetic permeability [8,9]. The idea of materials with negative refractive index [10] opens up new conceptual paradigms in photonics such as the idea of a perfect lens that goes beyond the diffraction limit resolution [11]. So far, very few experimental demonstrations of negative refraction in PCs in the near-IR frequency region have been carried out. The substitution of the SRR by a pair of metal patches separated by a dielectric medium, besides being a simpler arrangement, may lead to the development of negative index materials suitable for optical wavelengths [12]. All of these phenomena turn these engineered materials into highly interesting subjects for developing optical technology. However, to design and/or pro-

pose technological efficient applications, intense experimental work to explore the vast parameter space that is involved in the fabrication of these composite materials is needed. Furthermore, the interpretation of experimental data as well as the definition of optima materials and designs for technological purposes call for a complementary quantitative theoretical investigation.

Owing to the technical difficulties in the engineering of PCs in two and three dimensions [13], reports of one-dimensional (1D) PCs composed by various materials abound in the literature [14]. To acquire a deeper theoretical understanding on the nature of the PBGs, in Sec. II of this paper, we have developed a general equation based on a transfer matrix technique, to study the photonic band structure as well as the symmetry properties of the electromagnetic field that propagates through a one-dimensional periodic array composed by two different layers characterized by refractive indices n_1 and n_2 which can take on positive as well as negative values. In Sec. III a thorough investigation on the band structure of a superlattice composed by alternating layers of positive and negative refractive indices is performed by using Drude-type frequency-dependent models of the dielectric response and magnetic permeability for the negative medium. Finally, Sec. IV presents a summary and conclusions of the results obtained in the present study.

II. THEORETICAL FRAMEWORK

Let us begin by writing the Maxwell equation for an electric field propagating through a linear, isotropic dielectric media

$$\nabla \times (\nabla \times \mathbf{E}) + \frac{\mu(\mathbf{r})\varepsilon(\mathbf{r})}{c^2} \frac{\partial^2 \mathbf{E}}{\partial t^2} - \frac{\nabla \mu(\mathbf{r})}{\mu(\mathbf{r})} \times (\nabla \times \mathbf{E}) = \mathbf{0}, \quad (1)$$

where $\varepsilon(\mathbf{r})$ and $\mu(\mathbf{r})$ are the position-dependent dielectric constant and magnetic permeability, respectively. Here we note that, in general, both ε and μ are frequency-dependent functions, and that, for simplicity, we omit the explicit dependence in the notation. For a monochromatic field of angular frequency ω of the form

$$\mathbf{E}(\mathbf{r}, t) = \mathbf{E}(\mathbf{r})e^{-i\omega t}, \quad (2)$$

Eq. (1) becomes

$$\nabla \times (\nabla \times \mathbf{E}) - \mu(\mathbf{r})\varepsilon(\mathbf{r})\left(\frac{\omega}{c}\right)^2 \mathbf{E} - \frac{\nabla\mu(\mathbf{r})}{\mu(\mathbf{r})} \times (\nabla \times \mathbf{E}) = \mathbf{0}. \quad (3)$$

Limiting now ourselves to the case of a 1D photonic crystal along the z direction, described by a periodic dielectric constant $\varepsilon(z+d)=\varepsilon(z)$ and a periodic magnetic permeability $\mu(z+d)=\mu(z)$, where d is the period, the dispersion relation $\omega(k)$ in the case of an in-plane linearly polarized electromagnetic field of the form $\vec{E}(z, t)=E(z)e^{-i\omega t}\hat{x}$ may be obtained from the following equation:

$$\frac{d}{dz}\left(\frac{1}{n(z)Z(z)}\frac{dE(z)}{dz}\right) = -\frac{n(z)\omega^2}{Z(z)c^2}E(z), \quad (4)$$

where $n(z)=\sqrt{\varepsilon(z)}\sqrt{\mu(z)}$ and $Z(z)=\sqrt{\mu(z)}/\sqrt{\varepsilon(z)}$ are the refractive index and impedance, respectively. For a photonic crystal composed of alternating layers of two different materials, Eq. (4) must be solved by assuming the continuity of both the electric field $E(z)$ and of the expression $\frac{1}{n(z)Z(z)}\frac{dE(z)}{dz}$, which means that the two-component function

$$\psi(z) = \begin{pmatrix} \psi_1 \\ \psi_2 \end{pmatrix} = \begin{pmatrix} E(z) \\ \frac{1}{nZ} \frac{dE}{dz} \end{pmatrix} \quad (5)$$

is continuous through the photonic structure. This condition may be conveniently written by means of a transfer matrix as

$$\psi(z) = M_i(z - z_0)\psi(z_0) \quad (6)$$

for each layer of the heterostructure, where i denotes the layer index, z and z_0 are in the same layer, and $M_i(z)$ is the corresponding transfer matrix,

$$M_i(z) = \begin{pmatrix} \cos\left(\frac{\omega|n_i|z}{c}\right) & \frac{n_i cZ_i}{|n_i| \omega} \sin\left(\frac{\omega|n_i|z}{c}\right) \\ -\frac{|n_i| \omega}{n_i cZ_i} \sin\left(\frac{\omega|n_i|z}{c}\right) & \cos\left(\frac{\omega|n_i|z}{c}\right) \end{pmatrix}, \quad (7)$$

with

$$\det M_i(z) = 1. \quad (8)$$

When the n_i refractive index in layer i is purely imaginary (which occurs when ε_i and μ_i have opposite signs), $|n_i|$ must be changed to $i|n_i|$ in Eq. (7) and the following equations. In what follows, we choose the origin of coordinates located at the center of a first slab of width a , with dielectric constant ε_1 and magnetic permeability μ_1 , and denote by b the width of the second slab of dielectric constant ε_2 and magnetic permeability μ_2 . One may then write that

$$\psi\left(\pm\frac{a+b}{2}\right) = T(\pm a, \pm b)\psi(0), \quad (9)$$

where

$$T(\pm a, \pm b) = M_2\left(\pm\frac{b}{2}\right)M_1\left(\pm\frac{a}{2}\right) = \begin{pmatrix} p(\omega) & \pm q(\omega) \\ \pm r(\omega) & s(\omega) \end{pmatrix}, \quad (10)$$

$$p(\omega) = +\cos\frac{b\omega|n_2|}{2c}\cos\frac{a\omega|n_1|}{2c} - \frac{Z_2|n_1|n_2}{Z_1n_1|n_2|}\sin\frac{b\omega|n_2|}{2c}\sin\frac{a\omega|n_1|}{2c}, \quad (11)$$

$$q(\omega) = +\frac{n_1 cZ_1}{|n_1| \omega}\cos\frac{b\omega|n_2|}{2c}\sin\frac{a\omega|n_1|}{2c} + \frac{n_2 cZ_2}{|n_2| \omega}\sin\frac{b\omega|n_2|}{2c}\cos\frac{a\omega|n_1|}{2c}, \quad (12)$$

$$r(\omega) = -\frac{|n_2| \omega}{n_2 cZ_2}\sin\frac{b\omega|n_2|}{2c}\cos\frac{a\omega|n_1|}{2c} - \frac{|n_1| \omega}{n_1 cZ_1}\cos\frac{b\omega|n_2|}{2c}\sin\frac{a\omega|n_1|}{2c}, \quad (13)$$

$$s(\omega) = +\cos\frac{b\omega|n_2|}{2c}\cos\frac{a\omega|n_1|}{2c} - \frac{Z_1|n_2|n_1}{Z_2n_2|n_1|}\sin\frac{b\omega|n_2|}{2c}\sin\frac{a\omega|n_1|}{2c}. \quad (14)$$

It should be noted here that $ps - qr = 1$. By using now the Bloch condition

$$\psi(z+d) = e^{ikd}\psi(z), \quad (15)$$

and Eqs. (9) and (10), where $d=a+b$ is the period and k is chosen within the first Brillouin zone of the photonic crystal, i.e., $-\pi/d \leq k \leq \pi/d$, one may obtain the secular equation

$$ps(1-\lambda)^2 - qr(1+\lambda)^2 = 0 \quad (16)$$

with $\lambda = e^{ikd}$, leading to the two following equivalent relations:

$$\cos^2\left(\frac{kd}{2}\right) = +p(\omega)s(\omega), \quad (17)$$

$$\sin^2\left(\frac{kd}{2}\right) = -q(\omega)r(\omega). \quad (18)$$

Of course, the solutions of either (17) or (18) determine the band structure of the photonic crystal. Another equation, equivalent to (17) and (18), is obtained by subtracting (17) from (18) and using (11)–(14),

$$2 \cos kd = 2 \cos \frac{\omega d a |n_1| - b |n_2|}{c d} - \left(\frac{Z_1 n_1 |n_2|}{Z_2 |n_1| n_2} + \frac{Z_2 |n_1| n_2}{Z_1 n_1 |n_2|} + 2 \right) \times \sin \frac{a\omega|n_1|}{c} \sin \frac{b\omega|n_2|}{c}. \quad (19)$$

It should be noted that equations (17)–(19) are general enough and may be used to investigate the properties of photonic crystals composed by two different materials with all sorts of refractive index configurations. In particular, if we take n_1 positive and n_2 negative in (19), this equation reduces

$$E(z) = \begin{cases} \psi_1(0) \left(\cos \frac{\omega|n_1|}{c} z + i \frac{\sin kd}{2qs} \frac{n_1 c Z_1}{|n_1| \omega} \sin \frac{\omega|n_1|}{c} z \right) & \text{for } -\frac{a}{2} < z < \frac{a}{2}, \\ \psi_1(0) \left[\left(p + i \frac{\sin kd}{2s} \right) \cos \frac{\omega|n_2|}{c} \left(z - \frac{d}{2} \right) + \frac{n_2 c Z_2}{|n_2| \omega} \left(r + i \frac{\sin kd}{2q} \right) \sin \frac{\omega|n_2|}{c} \left(z - \frac{d}{2} \right) \right] & \text{for } \frac{a}{2} < z < \frac{a}{2} + b, \end{cases} \quad (20)$$

$$E(z) = \begin{cases} \psi_2(0) \left(\frac{n_1 c Z_1}{|n_1| \omega} \sin \frac{\omega|n_1|}{c} z + i \frac{\sin kd}{2pr} \cos \frac{\omega|n_1|}{c} z \right) & \text{for } -\frac{a}{2} < z < \frac{a}{2}, \\ \psi_2(0) \left[\left(q + i \frac{\sin kd}{2r} \right) \cos \frac{\omega|n_2|}{c} \left(z - \frac{d}{2} \right) + \frac{n_2 c Z_2}{|n_2| \omega} \left(s + i \frac{\sin kd}{2p} \right) \sin \frac{\omega|n_2|}{c} \left(z - \frac{d}{2} \right) \right] & \text{for } \frac{a}{2} < z < \frac{a}{2} + b, \end{cases} \quad (21)$$

where $\psi_1(0)=E(0)$ is the electric field at the center of the first slab ($z=0$) and $\psi_2(0)$ is the second component in (5) also evaluated at $z=0$.

Equations (20) and (21) provide the electromagnetic modes in a single elementary cell of the direct photonic crystal. By using the Bloch condition (15) one may determine these modes in other elementary cells. Of course, expression (20) is useful when $q(\omega)$ and $s(\omega)$ are different from zero, while (21) is useful when both $p(\omega)$ and $r(\omega)$ are nonzero.

By considering a superlattice whose single cell is composed by air ($n_1=1$) and gallium arsenide (GaAs, $n_2 \approx 3.6$) one finds that, according to Eqs. (17) and (18), the maximum and minimum band values occur at the center and at the edge of the Brillouin zone (BZ) of the photonic crystal. These extrema are determined from equations $r(\omega)=0$ [$p(\omega)=0$] and $q(\omega)=0$ [$s(\omega)=0$] at the center (edge) of the BZ. Furthermore, Eqs. (17) and (18) and Eqs. (20) and (21) lead to the following symmetry properties of the electromagnetic modes: (i) at the BZ center ($k=0$), they are even functions of z when $r(\omega)=0$ and $q(\omega) \neq 0$, whereas they are odd functions when $r(\omega) \neq 0$ and $q(\omega)=0$; (ii) at the BZ edge ($k=\pm\pi/d$), these modes are even if $s(\omega) \neq 0$ and $p(\omega)=0$, whereas they are odd when $s(\omega)=0$ and $p(\omega) \neq 0$ [of course, in cases (i) and (ii) the bands do not touch each other]; (iii) the touching of the bands occurs for $r(\omega)=q(\omega)=0$ at the BZ center, and for $p(\omega)=s(\omega)=0$ at the BZ edge, so that the solutions are degenerate and the general solution has no definite parity. This degeneracy is a consequence of the following zero photonic band-gap conditions:

$$ak_1 = \frac{a\omega|n_1|}{c} = N_1 \pi \quad (22)$$

and

to the corresponding one reported by Li *et al.* [15], who obtained it by using a different procedure.

The corresponding solutions for the in-plane electric field are straightforwardly obtained by using Eqs. (5)–(7), which lead to the following equivalent expressions for the field:

$$bk_2 = \frac{b\omega|n_2|}{c} = N_2 \pi, \quad (23)$$

where N_1 and N_2 are integers. At the BZ center N_1 and N_2 are both even or both odd, whereas at the BZ edge N_1 and N_2 are of opposite parities. Alternatively, one may write these conditions as

$$a = N_1 \lambda_1 / 2 \quad (24)$$

and

$$b = N_2 \lambda_2 / 2, \quad (25)$$

$\lambda_i = \frac{2\pi c}{|n_i| \omega}$, which displays the underlying null-gap physics as one of interference effects [16,17], and has clear similarities with the corresponding [18] problem of null gaps in the electronic spectra of semiconductor superlattices.

Finally, a fundamental quantity in the understanding of several properties of a photonic crystal is the DOS which is obtained by calculating the number of allowed states for a given frequency ω , i.e., by performing the integral over the BZ and summing over all bands m ,

$$g(\omega) = \sum_m \int_{\text{BZ}} dk \delta[\omega - \omega_m(k)] = \sum_{m,i} \frac{1}{\left| \frac{d\omega_m(k)}{dk} \right|_{k=k_m^{(i)}}}, \quad (26)$$

where $k_m^{(i)}$ are the wave vector solutions of the equation

$$\omega - \omega_m(k_m^{(i)}) = 0. \quad (27)$$

III. NON-BRAGG GAPS

We now turn to the interesting case of a photonic structure with alternating and homogeneous layers of two different

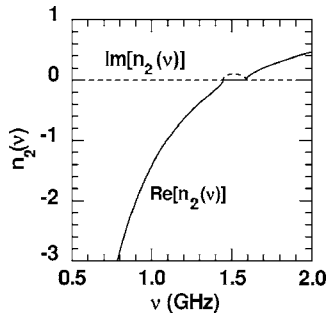


FIG. 1. Frequency-dependent refractive index according to the Drude's effective dielectric permittivity and magnetic permeability (see text).

materials with n_1 positive and independent of the frequency (here, for simplicity, we assume that the layer 1 material is air, i.e., $n_1=1$), and a layer 2 material with a frequency-dependent (homogeneous) $n_2(\omega)$ which may be negative within some frequency range. We shall limit ourselves to the case where the lattice spacing is much smaller than the wavelengths of the waves representing the electromagnetic field. Thus, the medium's response is essentially described by the layer 2 material parameters, i.e., by the $\varepsilon(\omega)$ dielectric permittivity and magnetic permeability $\mu(\omega)$, which we take as a Drude-type of response, based on the behavior of artificial metamaterials produced in the laboratories. By considering an array of wire elements with cuts periodically spaced, one has a material whose effective dielectric permittivity behaves as

$$\varepsilon(\omega) = \varepsilon - \frac{\alpha}{\omega^2}. \quad (28)$$

Analogously, a structure proposed by Pendry and colleagues [11], consisting of an array of splitted loops of conductor functioning according to Faraday's law as LC minicircuits, the SRRs, exhibits a magnetic permeability of the form

$$\mu(\omega) = \mu - \frac{\beta}{\omega^2}. \quad (29)$$

Experiments in the microwave region using metamaterials based on wires and SRR's indicate that they are frequency dispersive, exhibit narrow bandwidths and a considerable amount of loss. Based on these observations, we consider a layer 2 material modeled via a Drude-type effective dielectric permittivity and magnetic permeability, where one may choose [19,20] $\alpha=\beta=100$, $\varepsilon=1.21$, and $\mu=1.0$, with ω as the angular frequency in GHz. Here we point out that such effective dielectric permittivity and magnetic permeability may model a composite made of periodically LC loaded transmission lines [19]. In Fig. 1, the refractive index $n_2 = \sqrt{\varepsilon\mu}$ obtained from Eqs. (28) and (29) is plotted as a function of the frequency, and illustrates a negative branch attained when both ε and μ are negative, an imaginary portion in the case when ε and μ have opposite signs indicating evanescent behavior, and the usual well-known positive branch, for both ε and μ positive. In the case of alternating layers of positive and negative refraction indexes n_1 and n_2 ,

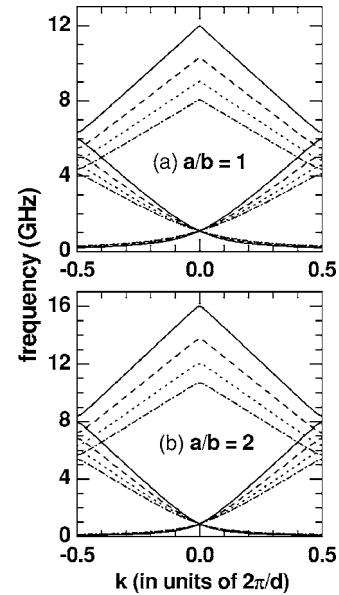


FIG. 2. Dispersion curves for (a) $\frac{a}{b}=1$ and (b) $\frac{a}{b}=2$. Solid, dashed, dotted, and dashed-dotted lines correspond to $a=12, 14, 16$, and 18 mm, respectively. In each case, three photonic bands only are shown around and above the $\langle n \rangle = 0$ gap.

respectively, one may use the following average:

$$\langle n(\omega_0) \rangle = \frac{1}{d} \int_0^d n(z, \omega_0) dz = \frac{an_1 - b|n_2(\omega_0)|}{d} = 0 \quad (30)$$

to define a ω_0 frequency which is the solution of

$$|n_2(\omega_0)| = \frac{a}{b} n_1. \quad (31)$$

It is then straightforward to show [21] that ω_0 corresponds to a forbidden frequency falling inside what is known as the “ $\langle n \rangle = 0$ gap.” Moreover, in contrast with what happens with the usual Bragg gaps [15], the value of ω_0 is independent of the size of the unit cell, and only depends on the $\frac{a}{b}$ ratio [of course, Eq. (31) implies that if the index contrast is high, one must have a high contrast in the widths to have a gap, whereas for low index contrast, one must have similar layer widths]. Figure 2 shows photonic bands around and above the $\langle n \rangle = 0$ gap for two different values of the ratio $\frac{a}{b}$, and various values of the width a of the first slab. Notice that the $k = \pm \pi/d$ higher gaps (between the second and third bands shown in Fig. 2) are usual Bragg gaps [15] due to the periodicity and folding back of bands, and with gap values dependent on the particular values of the a and b widths, i.e., on the size $d=a+b$ of the unit cell. For the two lower bands shown in Fig. 2, the same results are zoomed in Fig. 3, in which we have also plotted a line indicating the values of $\nu_0 = \omega_0/2\pi$ [cf. Eq. (31)] associated with the $\langle n \rangle = 0$ gap, which is now clearly seen.

Here we note that the above wave-vector-independent (long-wavelength limit) assumption of 1 and 2 homogeneous media described by constant (slab 1) and Drude-type (slab 2) frequency-dependent dielectric permittivity and magnetic

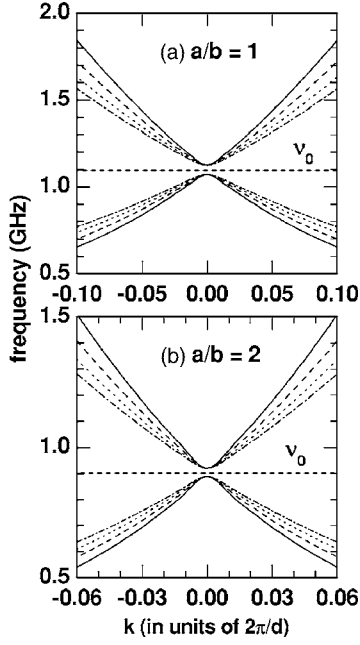


FIG. 3. Dispersion curves exhibiting the invariance of the $\langle n \rangle = 0$ gap for (a) $\frac{a}{b} = 1$ which opens around $\nu_0 = 1.1$ GHz and for (b) $\frac{a}{b} = 2$ which opens around $\nu_0 = 0.9$ GHz. Solid, dashed, dotted, and dashed-dotted lines correspond to $a = 12$ mm, 14, 16, and 18 mm, respectively.

permeability [Eqs. (28) and (29)], respectively, would imply that the wavelength of the radiation be much larger than the size of the unit cell, i.e., $\lambda_i = \frac{2\pi c}{|n_i|\omega} \gg a, b$. Provided that a and b are in the range discussed in Fig. 2 (i.e., a and b are in the range of $\approx 1-20$ mm), one may therefore show that, at the $k=0$ BZ center, the ν_- frequency, corresponding to the even solution associated with the top of the lower band around the $\langle n \rangle = 0$ gap in Fig. 3, is given by the solution of $r(\omega) = 0$ [see Eqs. (13) and (18) for $\lambda_i \gg a, b$], i.e.,

$$\frac{1}{\varepsilon(\omega)} = -\frac{b}{a}, \quad (32)$$

which results in [cf. Eq. (28)]

$$\nu_- = \frac{1}{2\pi} \sqrt{\frac{\alpha}{\left(\varepsilon + \frac{a}{b}\right)}}. \quad (33)$$

Similarly, one may show that the ν_+ frequency, corresponding to the odd solution associated with the bottom of the higher band around the $\langle n \rangle = 0$ gap in Fig. 3, is given by $q(\omega) = 0$ [see Eqs. (12) and (18) for $\lambda_i \gg a, b$] or

$$\frac{1}{\mu(\omega)} = -\frac{b}{a}, \quad (34)$$

resulting in [cf. Eq. (29)]

$$\nu_+ = \frac{1}{2\pi} \sqrt{\frac{\beta}{\left(\mu + \frac{a}{b}\right)}}. \quad (35)$$

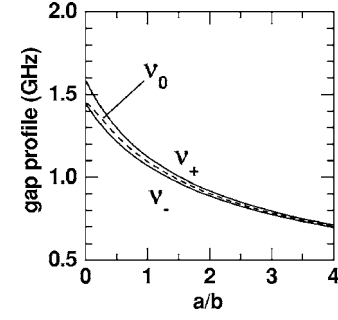


FIG. 4. Gap profile as a function of the ratio $\frac{a}{b}$. The broken line represents ν_0 at which $\langle n \rangle = 0$ and the full curves are the top (ν_-) or bottom (ν_+) of the first or second photonic bands in Fig. 3.

Notice that, as it happened with the ν_0 frequency associated with the $\langle n \rangle = 0$ gap, both ν_- and ν_+ are only dependent on the $\frac{a}{b}$ ratio [cf. Eqs. (33) and (35)]. In that respect, Fig. 4 displays the gap profile as a function of the relative layer width, i.e., the $\frac{a}{b}$ dependence of ν_0 , and of the ν_- or ν_+ frequencies corresponding to the top or bottom of the first or second photonic bands displayed in Fig. 3. Here we note that a full calculation with Eq. (18) gives essentially the same results as in Fig. 4, provided that a and b are in the range of $\approx 1-20$ mm.

In the following, for comparison purposes, we use another type of dispersion for both ε and μ , that is [15],

$$\varepsilon(\nu) = 1 + \frac{5^2}{0.9^2 - \nu^2} + \frac{10^2}{11.5^2 - \nu^2}, \quad (36)$$

$$\mu(\nu) = 1 + \frac{3^2}{0.902^2 - \nu^2}, \quad (37)$$

where ν is the frequency measured in GHz. Figure 5 illustrates the corresponding index of refraction behavior in the same fashion as it was done in Fig. 1 for the Drude-type response. Furthermore, Figs. 6 and 7 display the associated dispersion curves and gap profile [cf. Eqs. (32) and (34)], which should be compared with the corresponding Drude-type results of Figs. 2-4. Note that, although different dispersions were used for the effective dielectric permittivity

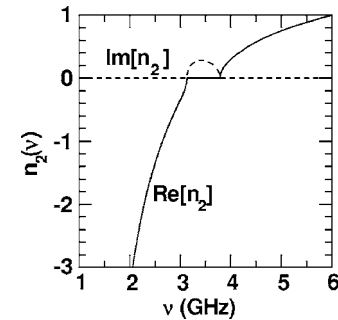


FIG. 5. Frequency-dependent refractive index associated to the effective dielectric permittivity and magnetic permeability used by Li *et al.* [15].

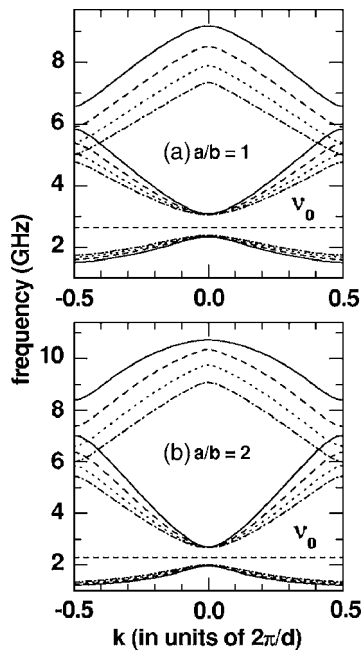


FIG. 6. Dispersion curves (three bands only, around the $\langle n \rangle = 0$ gap, are shown) associated with the refractive index depicted in Fig. 6, for (a) $\frac{a}{b} = 1$ and (b) $\frac{a}{b} = 2$. Solid, dashed, dotted, and dashed-dotted lines correspond, respectively, to the following values of a : $a = 12, 14, 16$, and 18 mm.

and magnetic permeability, calculated results show up, as expected, essentially the same physics.

IV. CONCLUSIONS

We have analyzed the band structure and density of states of 1D periodic arrays composed by two layers of refractive indexes n_1 and n_2 , which may take on positive as well as negative values. Within a transfer-matrix formalism, we have obtained photonic band structures, density of states and electromagnetic profiles. We have found new features and con-

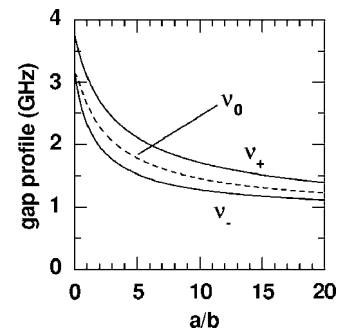


FIG. 7. Gap profile as a function of the ratio $\frac{a}{b}$. The broken line represents ν_0 at which $\langle n \rangle = 0$ and the full curves are the top (ν_-) or bottom (ν_+) of the first or second photonic bands in Fig. 6.

firmed predicted ones that are inherent to optical phenomena involving the propagation of light, i.e., null-gap points that appear whenever the optical path lengths within each layer are commensurate. In that respect, we have found a generalized condition closely related to the well-known occurrence of the so-called Bragg mirrors. Finally, we have characterized non-Bragg gaps [see conditions in Eqs. (32) and (34)], i.e., gaps that do not exhibit the usual Bragg sensitivity to cell sizes and that show up in frequency regions in which the average refractive index is null. Of course, as these are induced by an averaged effect, the notion of non-Bragg gaps should be extended to a higher class of inhomogeneous materials, as long as the inhomogeneities occur on length scales much smaller than the wavelength of the radiation, but large compared with atomic or molecular length scales.

ACKNOWLEDGMENTS

The authors would like to thank the Brazilian Agencies CNPq, FAPESP, Rede Nacional de Materiais Nanoestruturados/CNPq, MCT-Millennium Institute for Quantum Information, and MCT-Millennium Institute for Nanotechnology for partial financial support. Two of the authors (M.dD.-L. and E.R.G.) are thankful for the warm hospitality of the Institute of Physics of the State University of Campinas (Brazil), where part of this work was performed.

-
- [1] E. Yablonovitch, *Phys. Rev. Lett.* **58**, 2059 (1987).
 [2] S. John, *Phys. Rev. Lett.* **58**, 2486 (1987).
 [3] A. Blanco, E. Chomski, S. Grabtchak, M. Ibisate, S. John, S. W. Leonard, C. Lopez, F. Meseguer, H. Míguez, J. P. Mondia, G. A. Ozin, O. Toader, and H. M. van Driel, *Nature (London)* **405**, 437 (2000).
 [4] Yu. A. Vlasov *et al.*, *Nature (London)* **414**, 289 (2001).
 [5] P. Lodahl, A. Floris van Driel, I. S. Nikolaev, A. Irman, K. Overgaag, D. Vanmaekelbergh, and W. L. Vos, *Nature (London)* **430**, 654 (2004).
 [6] D. Mogilevtsev, S. Kilin, and S. B. Cavalcanti, *Photonics Nanostruct. Fundam. Appl.* **3**, 28 (2005).
 [7] V. G. Veselago, *Sov. Phys. Usp.* **10**, 509 (1968).
 [8] J. B. Pendry, A. J. Holden, W. J. Steward, and I. Youngs, *Phys. Rev. Lett.* **76**, 4773 (1996); J. B. Pendry, A. J. Holden, D. J. Robbins, and W. J. Steward, *IEEE Trans. Microwave Theory Tech.* **47**, 2075 (1999).
 [9] D. R. Smith, W. J. Padilla, D. C. Vier, S. C. Nemat-Nasser, and S. Schultz, *Phys. Rev. Lett.* **84**, 4184 (2000); R. A. Shelby, D. R. Smith, and S. Schultz, *Science* **292**, 77 (2001).
 [10] S. A. Ramakrishna, *Rep. Prog. Phys.* **68**, 449 (2005).
 [11] J. B. Pendry, *Phys. Rev. Lett.* **85**, 3966 (2000); *Contemp. Phys.* **45**, 191 (2004); J. B. Pendry and D. R. Smith, *Phys. Today* **57**(6), 37 (2004), and references therein.
 [12] C. M. Soukoulis, *Opt. Photonics News* **17**, 16 (2006).
 [13] S. G. Johnson and J. D. Joannopoulos, *Photonic Crystals: The Road from Theory to Practice* (Kluwer, Boston, 2002).
 [14] A. Yariv and P. Yeh, *Optical Waves in Crystals* (Wiley, New York, 1984), Chap. 6, and references therein.
 [15] J. Li, L. Zhou, C. T. Chan, and P. Sheng, *Phys. Rev. Lett.* **90**, 083901 (2003).
 [16] T. F. Krauss and R. M. De la Rue, *Prog. Quantum Electron.*

- 23**, 51 (1999).
- [17] S. B. Cavalcanti, M. de Dios-Leyva, E. Reyes-Gómez, and L. E. Oliveira, *Phys. Rev. B* **74**, 153102 (2006).
- [18] M. de Dios-Leyva, J. Sabin, and J. López-Gondar, *Phys. Status Solidi B* **134**, 615 (1986).
- [19] G. V. Eleftheriades, A. K. Yyer, and P. C. Kremer, *IEEE Trans. Microwave Theory Tech.* **50**, 2702 (2002).
- [20] A. Grbic and G. V. Eleftheriades, *J. Appl. Phys.* **92**, 5930 (2002); L. Liu, C. Caloz, C. C. Chang, and T. Itoh, *ibid.* **92**, 5560 (2002); H. Jiang, H. Chen, H. Li, Y. Zhang, and S. Zhu, *Appl. Phys. Lett.* **83**, 5386 (2003).
- [21] At the ω_0 frequency, Eq. (18) yields $\sin^2\left(\frac{kd}{2}\right) = \frac{1}{4}\left(1 - \frac{Z_2}{Z_1}\right) \times \left(1 - \frac{Z_1}{Z_2}\right) \sin^2\left(\frac{an_1\omega_0}{c}\right)$. As the right-hand side of the preceding equation is negative, provided that $\frac{an_1\omega_0}{c}$ is not an integral multiple of π , it implies that ω_0 is a forbidden frequency and falls within a photonic gap.